Supporting information

Dual-Functional Analogous cis-Platinum Complex with High Antitumor Activities and Two-Photon Bioimaging

Qiong Zhang,† Xiaohe Tian,¶ Guiju Hu,† Pengfei Shi,† Jieying Wu*,† Shengli Li,† Hongping Zhou,† Bao-Kang Jin,† Jiaxiang Yang,† Shengyi Zhang,† Yupeng Tian*,†

† *Key Laboratory of Functional Inorganic Materials Chemistry of Anhui Province, Department of Chemistry, Anhui University, Hefei, 230039, P. R. China*

¶*Department of Chemistry, The MRC/UCL Centre for Medical Molecular Virology, University College London, London,WC1H 0AJ, UK*

**Corresponding author, E-mail: jywu1957@163.com yptian@ahu.edu.cn*

Synthesis. The structures and synthesis routes of ligand **TSD** are shown in Scheme S1. The detailed synthetic procedures are described as follow of N-(4-nitrophenyl), N'-(4-ethoxyphenyl)phenylamine(**M1**), 4-((4′- ethoxyphenyl)(4″- nitrophenyl)amino) benzaldehyde (**M2**), 4-(4′-(diethyl amino)styryl)-N-(4″-ethoxyphenyl)-N-(4‴-amino phenyl) phenylamine (**M4**). 4-(4′-(diethyl amino)styryl)-N-(4″-ethoxyphenyl)-N-(4‴- pyridine carboxaldehyde amino phenyl) phenylamine(**TSD**), and complex **TDPt**. 4-(4′-(diethyl amino)styryl)-N-(4″- ethoxyphenyl)-N-(4‴-nitrophenyl) phenylamine (M3) was synthesized according to the literature[1].

N-(4-nitrophenyl), N'-(4-ethoxyphenyl)phenylamine(M1)

A suspension of 1.97 g(15 mmol) of paranitroanilinum, 2.48 g (10 mmol) of 4-Iodophenetole, then 2.76 g (20 mmol) of anhydrous K_2CO_3 and 30 mL DMSO were added into a three-necked flask equipped with a magnetic stirrer, a reflux condenser, and a nitrogen input tube, and then 0.23 g of L-proline and 0.19 g CuI were added slowly. The reaction mixture was refluxed for 9 h at 100ºC under nitrogen and monitored by TLC. After completion of the reaction, the mixture was washed by water, and then 200 mL of ethyl acetate was added, the organic layer separated, and dried with anhydrous sodium sulfate. The crude product was obtained as brown oil after removing the solvent. The crude product was purified by column chromatography with petroleum (b.p. 60-90 ºC) /ethyl acetate (5:1 by volume) to orange crystal. Yield: 65 %. ^{1}H NMR: (400 MHz, d_6-DMSO), δ(ppm): 8.18(s, 1H), 8.06(d, J = 8.0 Hz, 2H), 7.22(d, J = 8.0 Hz, 2H), 6.96(q, J = 8.0 Hz, 4H), 4.06(q, J = 6.8 Hz, 2H), 1.37(t, J = 6.8 Hz, 3H).

4-((4′- ethoxyphenyl)(4″- nitrophenyl)amino) benzaldehyde (M2)

3.72g (30 mmol) of 4-fluorobenzaldehyde, 2.60 g (10 mmol) of **M1**, 2.0 g (15 mmol) of anhydrous K_2CO_3, and two drops of Aliquate-336 were introduced into a round-bottom flask fitted with a condenser. The mixture was stirred at 90ºC for 72 h, and after cooling to room temperature, it was poured into an ice–water mixture. The aqueous layer was extracted with dichloromethane and the organic layer washed twice with cold water. After solvent evaporation, the dark red oil crude product was purified by column chromatography with petroleum (b.p. 60-90 ºC) /ethyl acetate (6:1 by volume) to orange crystal. Yield: 80 %. ^{1}H NMR (400 MHz, d_6-DMSO), δ(ppm): 9.90(s, 1H), 8.18 (d, J = 9.2 Hz, 2H), 7.85(d, J = 8.4 Hz, 2H), 7.25(d, J = 8.4 Hz, 2H), 7.22(d, J = 9.2 Hz, 2H), 7.05(q, J = 7.2 Hz, 4H), 4.06(q, J = 7.2 Hz, 2H), 1.35(t, J = 7.2 Hz, 3H).

4-(4′-(diethyl amino)styryl)-N-(4″- ethoxyphenyl)-N-(4‴- nitrophenyl) phenylamine (M3)

Red oil was obtained. Yield : 75 %. ^{1}H NMR (400 MHz, d_6-DMSO), δ(ppm): 8.05 (d, J = 9.2 Hz, 2H), 7.60(d, J = 8.4 Hz, 2H), 7.39(d, J = 9.2 Hz, 2H), 7.21(d, J = 8.8 Hz, 4H),7.08(d, J = 16 Hz, 1H), 7.01(d, J = 8.4 Hz, 2H), 6.92(d, J = 16 Hz, 1H), 6.70(q, J = 9.2 Hz, 4H), 4.04(q, J = 7.2 Hz, 2H), 3.35(q, J = 8.1 Hz, 4H), 1.34(t, J = 7.2 Hz, 3H), 1.10(t, J = 8.1 Hz, 6H).

4-(4′-(diethyl amino)styryl)-N-(4″-ethoxyphenyl)-N-(4‴-amino phenyl) phenylamine (M4)

A solution of 2.0 g (4 mmol) of **M3** dissolved in 50 mL ethanol was added into a round-bottom flask equipped with a magnetic stirrer and heated at 80 ºC. Then 0.45 g of Pd/C catalyst was added into the preceding reaction system and a solution of 7.0 mL of 85% hydrazine hydrate was added dropwise for about 0.5 h. The reactionwas monitored by TLC. After the completion of the reaction, the reaction mixture was filtered immediately and the solvent evaporation. Then the yellow oil crude product was purified by column chromatography with petroleum (b.p. 60-90 ºC) /ethyl acetate (6:1 by volume) to orange crystal. Yield: 72 %. IR (KBr, cm^{-1}) selected bands: 3458(m), 3372(s), 2976(s), 2919(w), 1607(s), 1505(s), 1399(m), 1267(s), 1235(s), 1194(m), 1053(m),822(m), 563(m), 521(m). ^{1}H NMR (400 MHz, d_6-DMSO), δ(ppm): 7.34 (d, J = 8.8 Hz, 2H), 7.26(d, J = 8.8 Hz, 2H), 7.02(d, J = 8.8 Hz, 2H), 6.93(d, J = 8.8 Hz, 4H), 6.87(d, J = 8.4 Hz, 1H), 6.82(q, J = 16 Hz, 2H), 6.78(d, J = 8.8 Hz, 2H), 6.67(d, J = 8.4 Hz, 2H), 6.60(d, J = 8.4 Hz, 2H), 5.26(s, 2H), 3.98(q, J = 7.2 Hz, 2H), 3.35(q, J = 7.2 Hz, 4H), 1.39(t, J = 7.2 Hz, 3H), 1.16(t, J = 7.2 Hz, 6H). EI-MS: m/z: 477.

4-(4′-(diethyl amino)styryl)-N-(4″-ethoxyphenyl)-N-(4‴- pyridine carbox aldehyde amino phenyl) phenylamine(TSD)

1.43 g (3 mmol) of **M4**, 0.32g (3 mmol) of 2-pyridine carboxaldehyde, and 15 ml ethanol were introduced into a round-bottom flask fitted with a condenser. The mixture was refluxed for 4 h, cooled to room temperature, after completion of the reaction, and then 20 mL of ethyl acetate was added, the organic layer separated, and dried with anhydrous sodium sulfate. Then the yellow oil crude product was purified by column chromatography with petroleum (b.p. 60-90 ºC) /ethyl acetate (6:1 by volume) to orange crystal. Yield: 81%. IR (KBr, cm^{-1}) selected bands: 3445(w), 2971(m), 2927(m), 1606(s), 1500(s), 1239(s), 823(s), 540(w), 526(w). ^{1}H NMR (400 MHz, d_6-DMSO), δ(ppm): 8.70 (d, J = 6.0 Hz, 1H), 8.64(s, 1H), 8.13 (d, J = 8.0 Hz, 1H), 7.93 (t, J = 8.0 Hz, 1H), 7.50 (t, J = 6.0 Hz, 1H), 7. 43 (d, J = 8.4 Hz, 2H), 7.35(q, J = 8.4 Hz, 4H), 7.07(d, J = 8.4 Hz, 2H), 7.00(q, J = 8.4 Hz, 4H), 6.90(q, J = 16 Hz, 2H), 6.64(d, J = 8.4 Hz, 2H), 4.02(q, J = 7.2 Hz, 2H), 3.30(q, J = 7.2 Hz, 4H), 1.34(t, J = 7.2 Hz, 3H),

1.09(t, J = 7.2 Hz, 6H). ^{13}C NMR (400 MHz, d-$CHCl_3$), δ(ppm): 156.3, 153.7, 151.6, 146.7, 146.3, 145.2, 138.5, 135.2, 133.1, 130.7, 128.5, 127.1, 126.0, 125.3, 124.5, 123.8, 122.4, 121.9, 120.2, 117.3, 112.6, 111.5, 69.4, 44.6, 15.8, 14.2. EI-MS: m/z: 566 ([M^+]).

Complex TDPt

0.28 g (0.5 mmol) of **TSD**, 0.21 g (0.5 mmol) of $K_2[PtCl_4]$, and 50 ml mixed solvent (acetonitrile and water (v/v = 1:1)) were introduced into a round-bottom flask fitted with a condenser. The mixture was refluxed for 16 h, the part of solvent evaporation, after completion of the reaction, filtered off, and washed with petroleum, water and ethnol. Then 0.39g the brown powder was obtained, Yield: 89%. FT-IR (parafilm, cm^{-1}) selected bands: $\upsilon_{Pt\text{-}Cl}$ 338, $\upsilon_{Pt\text{-}N}$ 519. ^{1}H NMR (400 MHz, d_6-DMSO), δ(ppm): 9.34 (d, J = 6.0 Hz, 2H), 8.24(d, J = 8.0 Hz, 1H), 7.93 (m, 2H), 6.95 (m, 17H), 4.00(q, J = 7.2 Hz, 2H), 3.33(q, J = 7.2 Hz, 4H), 1.31(t, J = 7.2 Hz, 3H), 1.07(t, J = 7.2 Hz, 6H). ^{13}C NMR (400 MHz, $CDCl_3$), δ(ppm): 165.8, 156.3, 151.6, 146.7, 146.3, 145.2, 138.5, 135.2, 133.1, 130.7, 128.5, 127.1, 126.0, 125.3, 124.5, 123.8, 122.4, 121.9, 120.2, 117.3, 112.6, 111.5, 69.4, 44.6, 15.8, 14.2. Elemental analysis calcd (%) for $C_{38}H_{38}Cl_2N_4OPt$: C, 54.81, H, 4.60, N, 6.73, O, 1.92. Found: C, 55.27, H, 4.16, N, 7.25, O, 2.35. ^{195}Pt NMR[500MHz, d_6-DMSO, δ]: -2304 ppm. ESI-MS: m/z: cal: 832.2, found: 834.

Experiment

Materials and Apparatus. All solvents were dried and purified by usual methods. Elemental analysis was performed with a Perkin-Elmer 240B analyzer. IR spectra (4000-400 cm^{-1}), as KBr pellets, were recorded on a Nicolet FT-IR-870 SX spectrophotometer. The ESI mass spectra were obtained on a Finnigan LCQ Spectrometer. ^{1}H and ^{13}C NMR spectra were performed on Bruker 400 spectrometer with TMS as the internal standard.

Structure Investigation. The detailed synthesis procedures of ligand **TSD** are described in the Supporting Information, and **TDPt** is synthesized by general method (shown in Scheme 1). The resulting brownish complex is air-stable; was characterized by ^{1}H, ^{13}C, and ^{195}Pt NMR spectroscopy, positive-ion ESI-MS, and far-IR spectroscopy, and gave satisfactory elemental analyses. The far-IR of **TDPt** (Figure S1 in the supporting information) exhibits a band assigned to ν(Pt-Cl) at 338 cm^{-1}, and ν(Pt-N) at 519 cm^{-1}. The ESI-MS spectra of TDPt showed a positive peak at m/z value of 834.4 (supporting information Figure S2), which can be assigned to [Pt (TSD)Cl_2+H^+]. The chemical shifts of $\delta_{\text{-N=CH-}}$ (9.006 ppm) in the ^{1}H NMR spectra of **TDPt** changed apparently to the lower field when compared with that of **TSD**(δ = 8.64), due to N atom

coordination to Pt. The ^{195}Pt-NMR spectrum for TDPt (supporting information Figure S3) exhibits a signal at -2304 ppm, as a clear evidence of the platinum atom in a $PtCl_2N_2$ coordination environment.[2]

Computational Details. Density functional theory calculations were employed to investigate photophysical properties of compounds **TSD** and **TDPt**. The calculated geometries were optimized at the B3LYP level. The LANL2DZ and 6-31G* basis sets were employed for the Pt(II) atom and the other atoms, respectively. All these calculations were accomplished by using the Gaussian 03 software package[3]. At the same level, time dependent density functional theory (TDDFT) has been employed to obtain excitation energies and oscillator strengths of the optimized structures. An analytical frequency analysis provides evidence that the calculated species represents a true minimum without imaginary frequencies on the respective potential energy surface. In the calculation of the optical absorption spectrum, the 25 lowest spin-allowed singlet-singlet transitions, up to energy of ~5 eV, were taken into account.

The two-photon absorption cross-section, which can be directly comparable with experimental results, is defined as:

$$\sigma_{tp} = \frac{4\pi^2 a_0^5 \alpha}{15 c_0} \frac{\omega^2 g(\omega)}{\Gamma_f} \delta_{tp}$$

Here α_0 is the Bohr radius, c_0 is the speed of light, α is the fine structure constant, ω is the photon frequency of the incident light, and $g(\omega)$denotes the spectral line profile, which is assumed to be a δ function here, Γ_f is the lifetime broadening of the final state, which is commonly assumed to be 0.1 eV[4], and σ_{tp} is orientation average value of the two-photon absorption probability in gas and solution, which is written as follows[5],

$$\delta_{tpa} = \sum_{\alpha\beta} \left[F \times S_{\alpha\alpha} S^*_{\beta\beta} + G \times S_{\alpha\beta} S^*_{\alpha\beta} + H \times S_{\alpha\beta} S^*_{\beta\alpha} \right]$$

where F, G, and H are coefficients dependent on the polarization of the light. $S_{\alpha\beta}$ is the two-photon transition matrix element. For the absorption of two photons with the same frequency $\omega_f / 2$ it can be written as[6],

$$\delta_{tpa} = \sum_{\alpha\beta} \left[F \times S_{\alpha\alpha} S^*_{\beta\beta} + G \times S_{\alpha\beta} S^*_{\alpha\beta} + H \times S_{\alpha\beta} S^*_{\beta\alpha} \right]$$

where ω_i and ω_f denote the excitation frequency of the intermediate state $|\, i \,\rangle$ and final state $|\, f \,\rangle$ respectively, $\alpha, \beta \in (x, y, z)$, and the summation goes over all the intermediate states including the ground state $|\, 0 \,\rangle$ and the final state $|\, f \,\rangle$.

The most straightforward approach to analyze optical properties of molecules is the response theory[7], which can provide an analytical solution for the 2PA cross-section. The equilibrium geometries of molecules in the gas phase are optimized by use of the Gaussian package[2 at the hybrid density functional theory (DFT/B3LYP) level with the 6-31G* basis set. The 1PA and 2PA properties are calculated by use of the response theory at the DFT level implemented in DALTON[8, 9].

One-Photon Spectroscopy. UV-vis absorption spectra were recorded on a SHIMADZU UV-3600 spectrophotometer using quartz cells with a path length of 5 mm. In all spectroscopic measurements, spectrophotometric grade solvents were used. Extinction coefficients (ε_{max}), λ_{max}, were determined on at least five solutions (toluene, ethyl acetate, ethanol, acetonitrile, DMF), obtained by dilution of two or three independent stock solutions and with concentrations spanning an order of magnitude or more. Fluorescence emission and excitation spectra were collected using a HITACHI F-2500 Spectro-fluorophotome and were fully corrected. Fluorescence quantum yields (Φ), λ_{flu}, were determined on optically dilute solutions. The measurements were performed relative to coumarin 307 in ethanol ($\Phi = 0.56$).

Fluorescence lifetime. For time-resolved fluorescence measurements, the fluorescence signals were collimated and focused onto the entrance slit of a monochromator with the output plane equipped with a photomultiplier tube (HORIBA HuoroMax-4P). The decays were analyzed by 'least-squares'. The quality bof the exponential fits was evaluated by the goodness of fit (χ^2).

Nonlinear Optical Properties (NLO) and Two-Photon Absorption (TPA) Cross-Section

Section change was monitored at this concentration. The TPA experiments were carried out on the open-aperture Z-scan setup.[10] All the optical studies were done using a femtosecond laser with a pulse duration of 140 fs and 80 MHz repetition rate. The thermal heating of the sample with high repetition rate (HRR) laser pulse was removed by the use of a mechanical chopper running at 1 kHz (see the Supporting Information).[11] The nonlinear absorption component was evaluated under an open aperture. The filled squares represent the

experimental data measured under this condition. It is clearly illustrated that absorption increases as the incident light irradiance rises. The solid line in Fig. 2 is the theoretical curve from the eq (1)-(3).[4]

$$T(z) = \frac{1}{q(z)\sqrt{\pi}} \int_{-\infty}^{+\infty} \ln[1 + q(z)] \exp(-\tau^2) d\tau \qquad (1)$$

$$q(z) = \beta I_0 L_{eff} / (1 + z^2/z_0^2) \qquad (2)$$

$$L_{eff} = (1 - e^{-\alpha L}) / \alpha \qquad (3)$$

where I_0 is the input intensity at the focus $z = 0$, L is the sample length, α is the linear absorption coefficient and β is the 2PA coefficient. $z_0 = \pi\omega_0^2/\lambda$ is the Rayleigh diffraction length, ω_0 is the radius of beam at focus. Thus, once an open-aperture *Z*-scan is performed, the nonlinear absorption coefficient β can be unambiguously deduced. The open-aperture transmittance is symmetric with respect to the focus ($z = 0$), where it has a minimum transmittance obviously. The intensity dependent transmittance indicates the nonlinear absorption for **TSD and TDPt**. For no linear absorption above 500 nm was observed in the linear absorption spectrum of all the compounds in DMF, we attribute the nonlinear absorption to the 2PA effect. Furthermore, the molecular TPA cross-section (σ) could be determined by using the following relationship:[12]

$$\sigma = h\gamma\beta / N_A d \times 10^{-3}$$

here h is the Planck's constant, γ is the frequency of input intensity, N_A is the Avogadro constant, and d is the concentration of the sample.

Cell Culture and the guidelines for use of commercial dyes. The human cervical carcinoma cells Hela, neuroblastoma cells (SH-SY5Y), stomach cancer cells (BGC823), human breast cancer cells (MCF-7) and human renal epithelial cell (293T) were seeded in six-well plates at a density of 105 cells per well and grown for 96 h used DMEM nutrient solution. For cytotoxicity assays and live-cell imaging, cell cultures were incubated with complex solution (20μM) and maintained at 37 ºC under 5% CO_2/95% air for 2 h of incubation time. The cells were then washed with PBS (3×3 mL per well), and PBS (3 mL) was added to each well. The commercial dyes (Syto9 (green), Lysotracker Yellow, Mitotracker Red (cyan) and DAPI was used in the co-localization system, the guidelines for use were download from Life Technologies (www.lifetechnologies.com)

In Vitro Cytotoxity Assays. The cytotoxicity of samples IC50 values were determined using the MTT assay, as described by Carmichael *et al.*[13], which makes use of the conversion of MTT [3-(4,5-dimethylthiazol-2-yl)-2,5-diphenyltetrazolium bromide] to a purple formazan product by the mitochondrial dehydrogenase of viable cells. Detailedly, the cells were seeded in a 96-well plate at a density of 5000 cells per well and incubated with 100 μL culture medium containing a series of doses of the samples at 37 °C for 48 h. After the incubation, the culture medium in each well was removed and the cells were washed three times with PBS. 20 μL of MTT solution (5 mg/mL) was added to each well and cultured for another 2h or 4 h. The supernatant was discarded and then 100 μL of DMSO was added to each well. The values of the plate were observed on a microplate reader at 570 nm (Safire, Tecan). The results were expressed as the viable percentage of cells after various treatments relative to the control cells without any treatment. IC50 values were determined as the drug concentration required to reduce the absorbance to 50% of that in the untreated, control wells.

Cytotoxicity Assays in Human renal epithelial cell (293T) Cells. To ascertain the cytotoxic effect of complex [Pt(**TSD**)Cl_2] treatment over a 24-h period, The cell viability (%) was calculated according to the following equation used MTT assays: cell viability % = $OD_{570(sample)}/OD_{570(control)}$ ×100, where $OD_{570(sample)}$ represents the optical density of the wells treated with various concentration of the compounds and $OD_{570(control)}$ represents that of the wells treated with DMEM + 10% FCS. Three independent trials were conducted, and the averages and standard deviations are reported. The reported percent cell survival values are relative to untreated control cells.

Microscopy. Cells were luminescently imaged on a Zeiss LSM 510 META upright confocal-laser scanning microscope with 40X and 63X water-dipping lenses. For complex, excitation energy of 800 nm was used and the fluorescence emission was measured at 450 nm. Costaining was performed by using SYTO9 (2 μM, Ex=488, Em=500–530 nm) for 10 min (in PBS), Lysotracker Yellow (75 nM, Ex=458, lem=500–560 nm) for 60 min (in growth medium), Mitotracker Deep-Red (50 nm, Ex=633, Em=650-700 nm) for 10 min (in PBS),. Image data were acquired and processed by using Zeiss LSM Image Browser, Zeiss LSM Image Expert and ImageJ. For TEM, MCF-7 cells were incubated with complex (2-4 h) then fixed by using 3% glutaraldehyde and dehydrated with ethanol. TEM samples were sectioned in Araldite resin by microtome and examined on a FEI Tecnai instrument operating at 80 kV equipped with a Gatan 1 k CCD Camera.

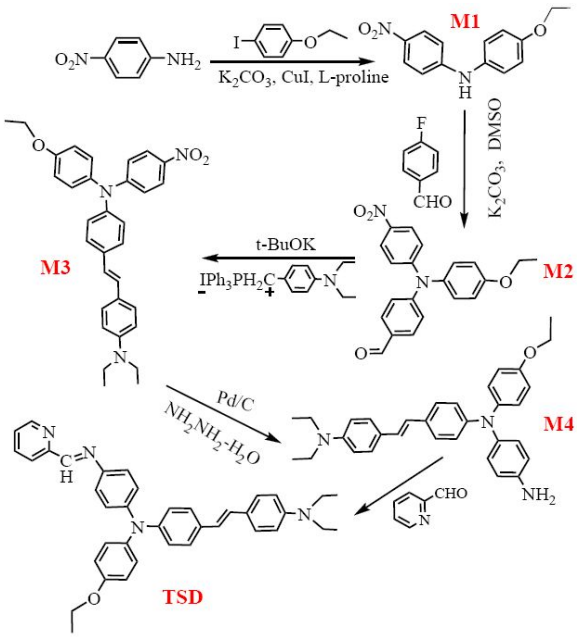

Scheme S1 Synthetic routes for the ligand.

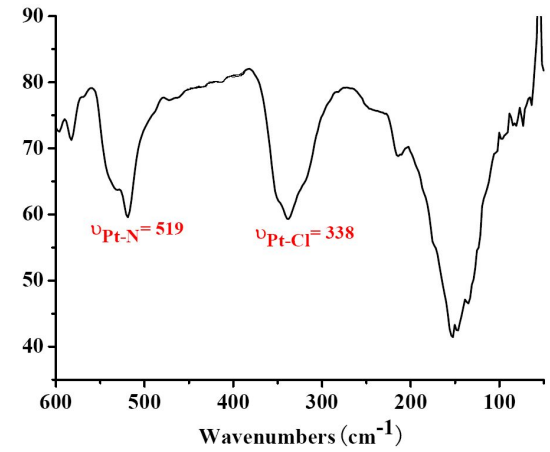

Figure S1 The Far-IR spectrum of complex **TDPt**

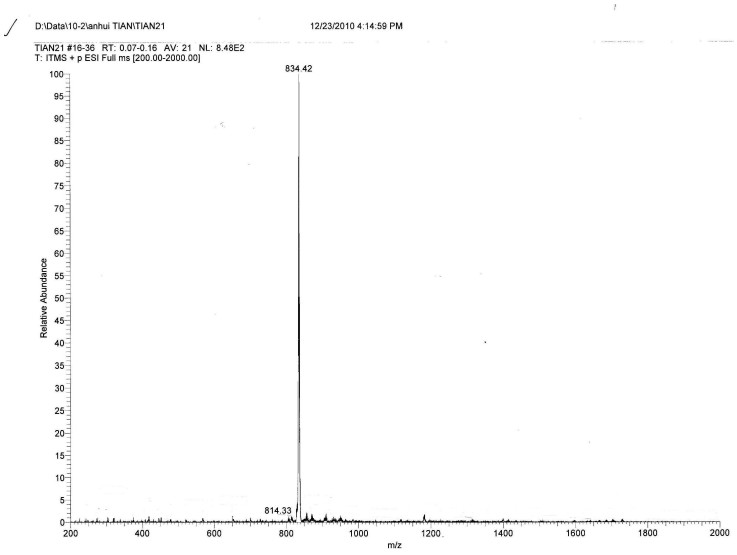

Figure S2 The ESI-MS spectrum of complex **TDPt**

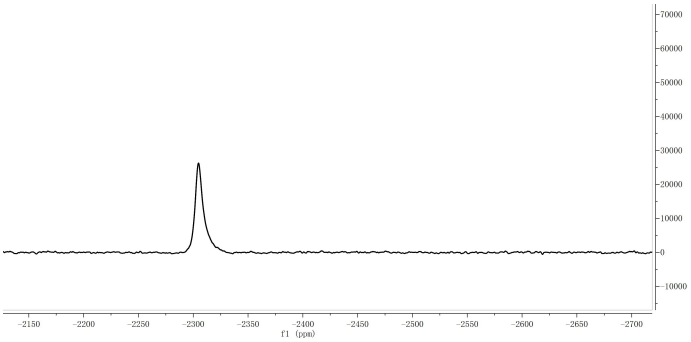

Figure S3 The ^{195}Pt-NMR spectrum of complex **TDPt**

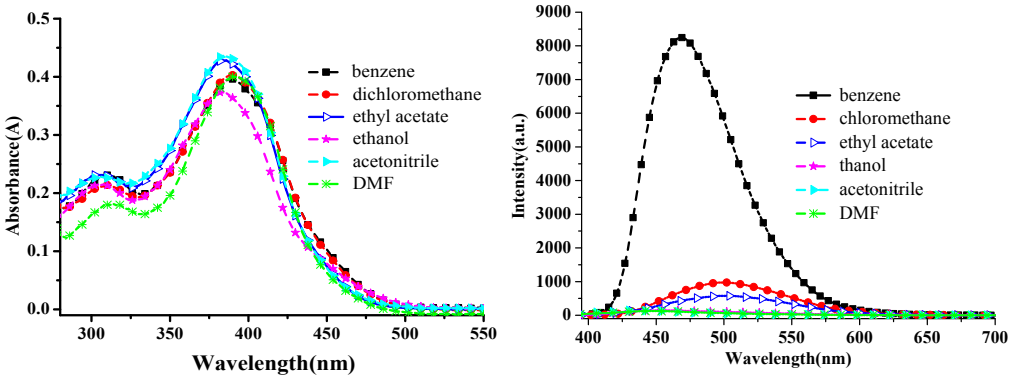

Figure S4 Linear absorption (left) and one-photon excited fluorescence (right) spectra of **TSD** in differents solution with 1×10^{-5}M.

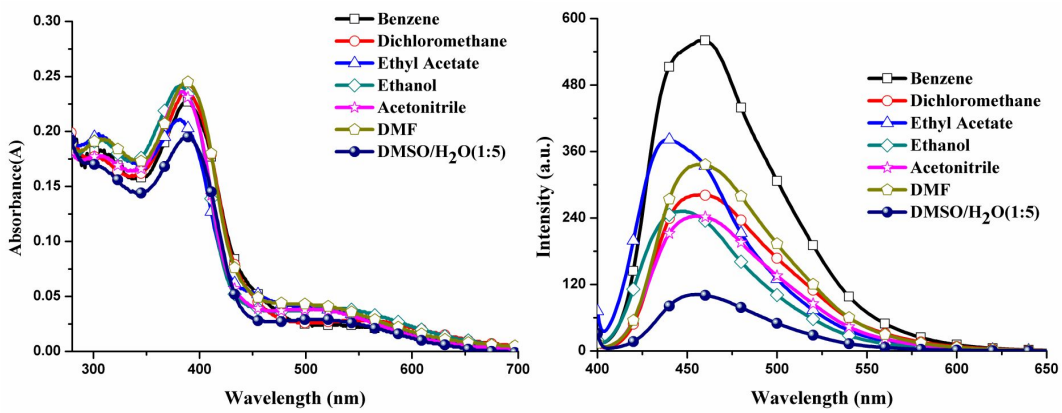

Figure S5 Linear absorption (left) and one-photon excited fluorescence (right) spectra of **TDPt** in different solvents with 1×10^{-5}M.

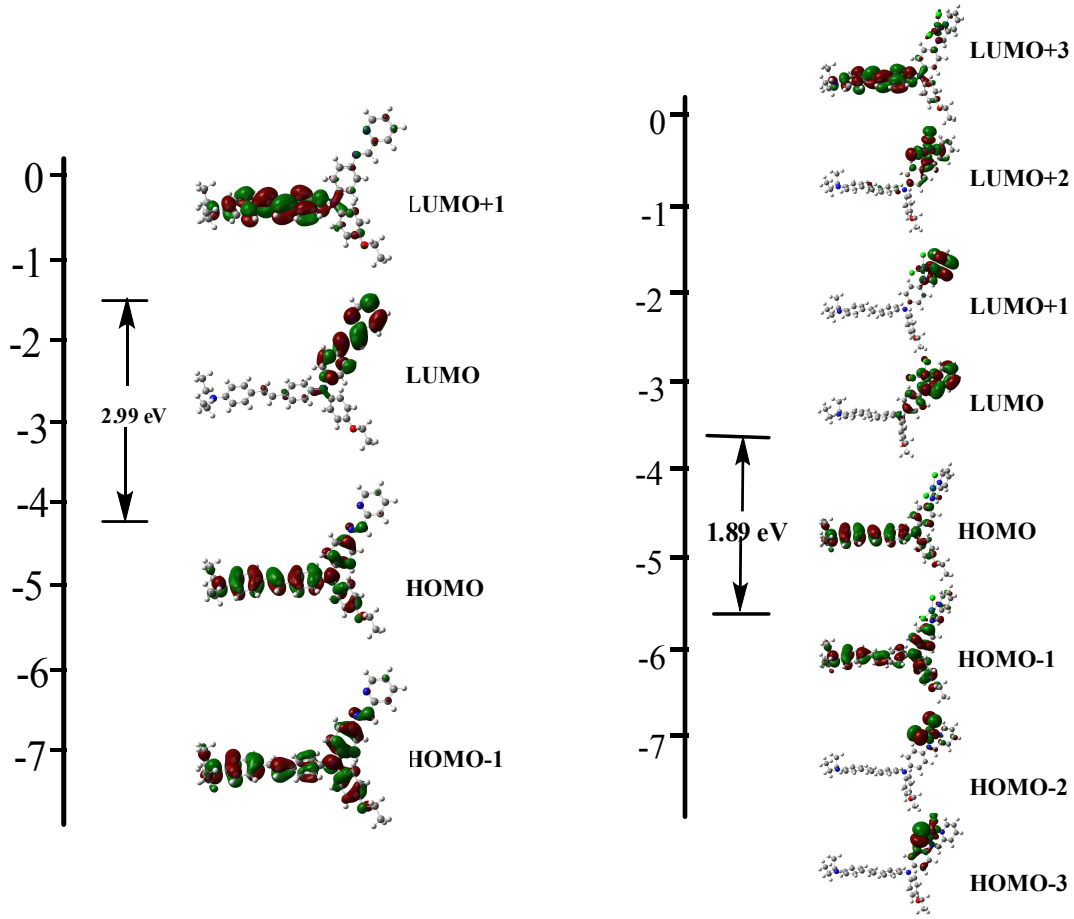

(a) **TSD** (b)**TDPt**

Figure S6 Electron density distributions of frontier orbitals of TSD(a) and TDPt(b)

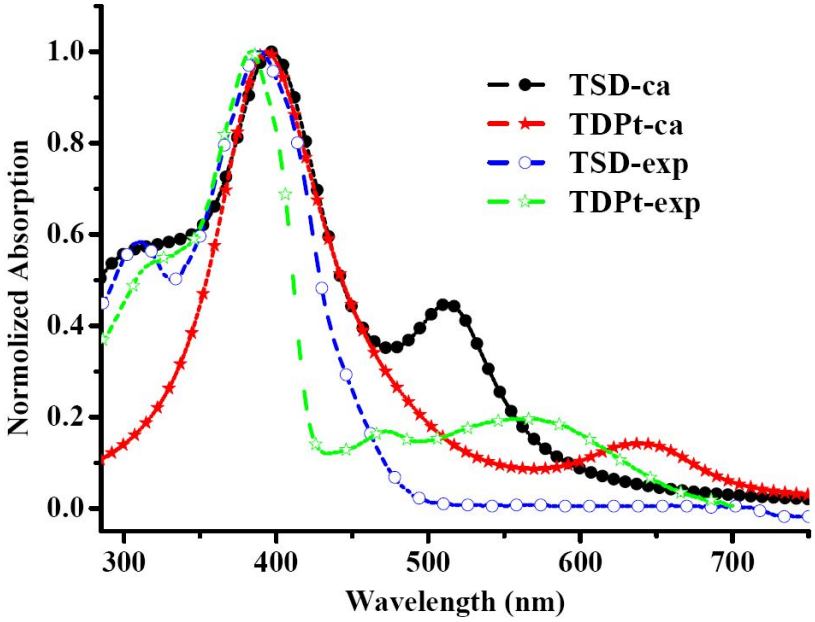

Figure S7 Experimental and simulated UV-Visible spectra of compounds **TSD** and **TDPt** (**TSD-ca** and **TDPt-ca** refering to experimental spectra, **TSD-exp** and **TDPt-exp** refering to simulated UV-Visible spectra).

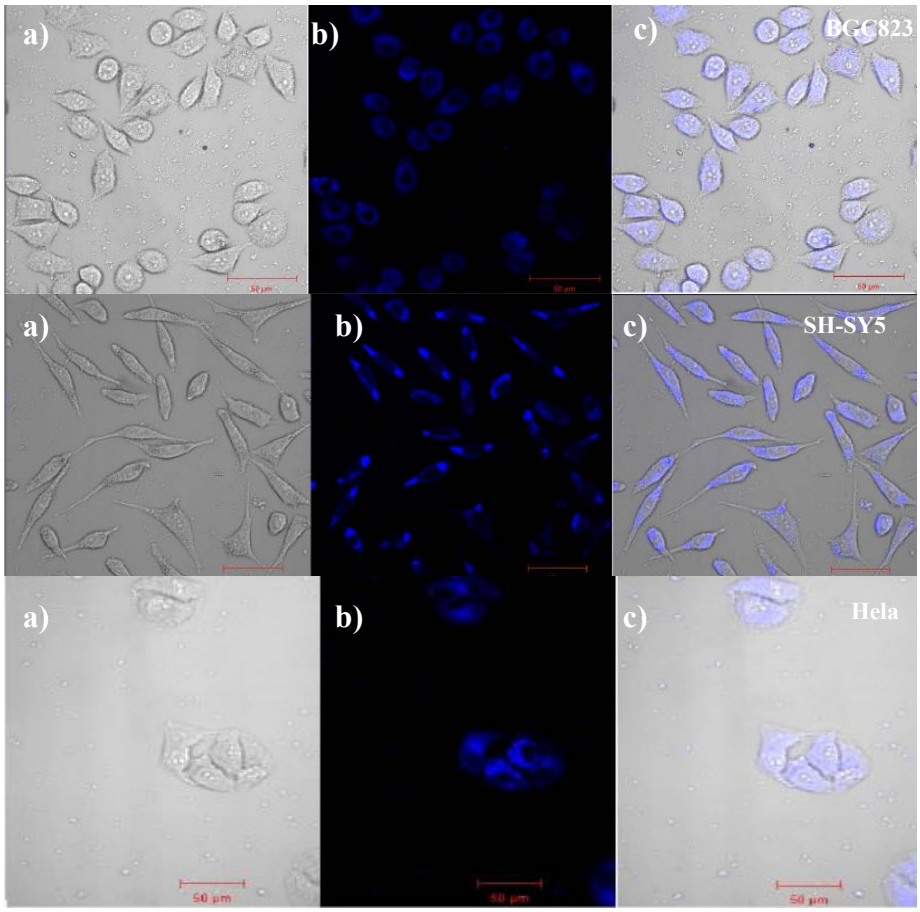

Figure S8 Confocal fluorescence imaging of **TDPt** with BGC823, SH-SY5Y and Hela cell lines. a) bright-field image of the cells stained with complex **TDPt**. b) Confocal fluorescence imaging of

the same cells with excitation at 400 nm. c) merged image.

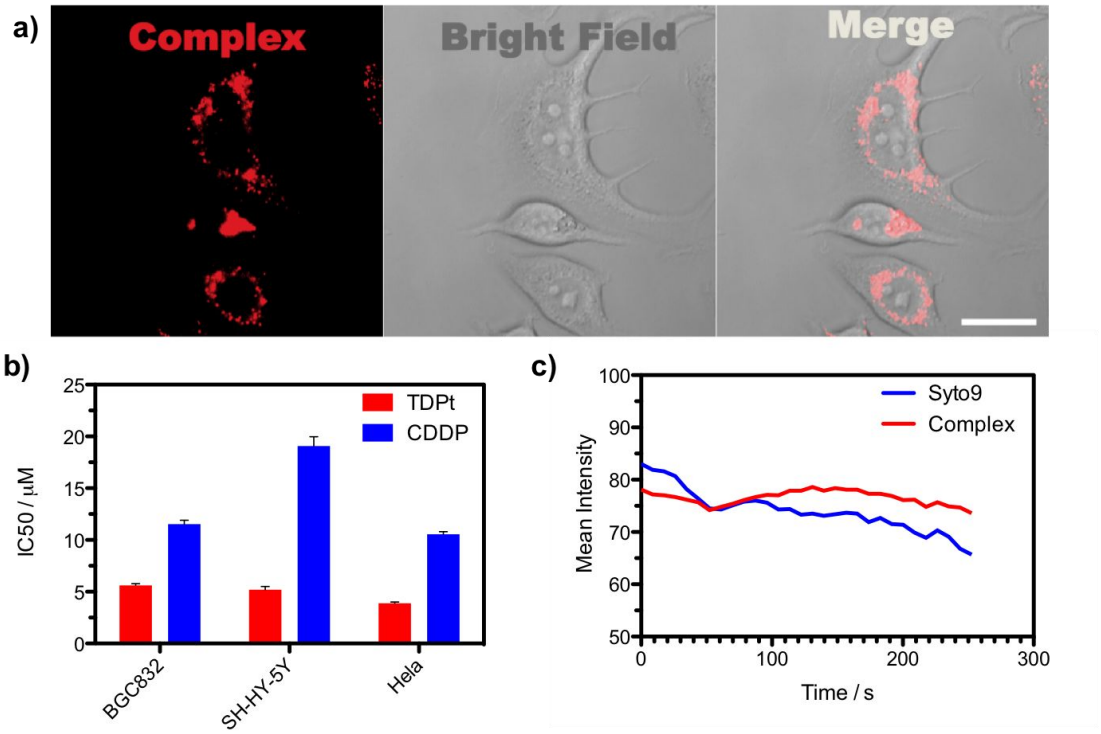

Figure S9 a) bright field image of MCF-7 incubated with complex. b) 24 hours IC_{50} of TDPt and CDDP on three types of cancer cells. c)Time series showing luminescence intensity of **TDPt** in a MCF-7 cell (200μM, 2hours incubation) under laser exposure over 15mins, compare with Syto 9.

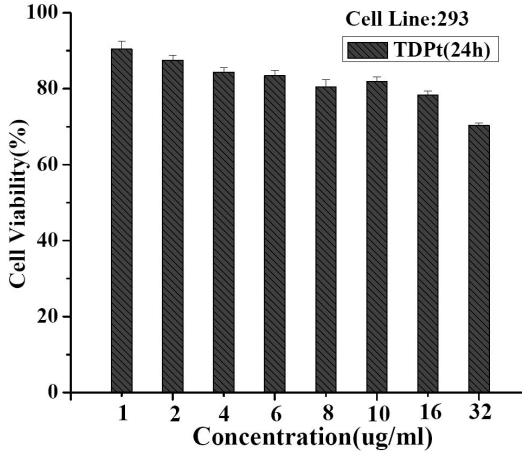

Figure S10 Toxicity of **TDPt** 293 cell lines.

Table S1 Photophysical properties of chromophores **TSD and TDPt** in several of different polar solvents

	solvent	$\varepsilon_{max}\times10^4$	λ_{max}^{abs}	λ_{max}^{SPEF}	Φ	τ (ns)	β^a	σ^b
TSD	Benzene	2.31, 3.96	310, 390	468	0.423	1.53		
	Dichloromethane	2.14, 4.03	310, 390	499	0.061	1.48		
	Ethyl acetate	2.31, 4.28	305, 386	502	0.038	1.43		
	Ethanol	2.15, 3.73	308, 384	454	0.011	1.38		
	Acetonitrile	2.28, 4.36	306, 384	435	0.008	1.41		
	DMF	1.81, 4.00	312, 392	446	0.008	1.31	0.0290	1800
TDPt	Benzene	2.70, 4.89,	315, 383, 570	461	0.030	1.46		
	Dichloromethane	--, 6.15, 1.19	--, 384, 566	458	0.010	1.54		
	Ethyl acetate	3.49, 6.57,	309, 378, 530	439	0.009	1.37		
	Ethanol	1.67, 2.59,	305, 380, 524	444	0.005	1.51		
	Acetonitrile	--, 9.34, 1.59	--, 380, 514	449	——	1.40		
	DMF	2.89, 5.12,	314, 388, 504	449	——	1.39	0.172	10651

λ_{max}^{abs} : max of the UV absorption spectra in nm, ε_{max} : The corresponding molar absorption coefficient, λ_{max}^{SPEF} : max of the SPEF spectra in nm. Φ Fluorescence quantum yield, τ: Fluorescence lifetime.

Table S2 Experimental and Calculated single- and two-photon-related photophysical properties of chromophores **TSD** and **TDPt** in gas phase.

Compounds	ΔE_1(eV)[a] /λ_{max}(nm)[b]	Character	OI[c]	f[d]	ΔE_2(eV)[e] /λ_{max}(nm)[f]	δ(GM)[g]	β (cm GW^{-1})(exp)	σ (GM)(exp)
TSD	2.99/415	π→π*/ICT	H-1 →L, H→ L+1	0.45	3.73/663	2090	0.00294	118
	3.16/392	π→π*/ ICT	H-1 →L,	1.03	--	--		
TDPt	1.89/654	MLCT	H-2 →L, H-1→ L	0.11	2.69/919	14212	0.029	1167
	2.85/410	MLCT	H-2→L+	0.23				
	3.04/407	MLCT	H-2→L+	0.16				
	3.16/392	MLCT	H-3→L+	0.16				
	3.19/387	LICT	H → L+3	0.88	--	--		

[a] The energy gap of the one-photon absorption band. [b] Peak position of the longest absorption band.[c] TDDFT Method with the Orbitals Involved (OI) [d] Only the singlet excited stated Oscillator Strengths with $f > 0.1$ were listed. [e] The energy gap of the two-photon absorption band. [f] Peak position of the two-photon absorption band. [g] Two-photon absorption cross section in GM (1 GM=10^{-50} cm^4 s photon^{-1}).

Table S3 IC_{50}(μM) for *Cis*-platin and complex **TDPt**

	BGC823		SH-SY5Y		Hela	
	24h	48h	24h	48h	24h	48h
TDPt	5.62	5.32	5.01	4.71	3.9	4.6
CDD	11.2	3.73	18.3	9.67	10.	5.0

References:

[1] C. Xu, W. W. Webb, *J Opt Soc Am B* **1996**, *13*, 481-491.

[2] a) Gao, J.; Woolley, F. R.; Zingaro, R. A.; *J. Med. Chem.* **2005**, *48,* 7192–7197; b) Teisser, C.; Rochon, F. D.; *Chim. Acta* **1999**, *295*, 25–38; c) Rochon, F. D.; Buculei, V. *Inorg. Chim. Acta* **2005**, *358*, 2040–2056.

[3] Frisch, M. J.; Trucks, G. W.; Schlegel, H. B.; Scuseria, G. E.; Robb, M. A.; Cheeseman, J. R.; Montgomery, J. A., Jr.; Vreven, T.; Kudin, K. N.; Burant, J. C.; Millam, J. M.; Iyengar, S. S.; Tomasi, J.; Barone, V.; Mennucci, B.; Cossi, M.; Scalmani, G.; Rega, N.; Petersson, G. A.; Nakatsuji, H.; Hada, M.; Ehara, M.; Toyota, K.; Fukuda, R.; Hasegawa, J.; Ishida, M.; Nakajima, T.; Honda, Y.; Kitao, O.; Nakai, H.; Klene, M.; Li, X.; Knox, J. E.; Hratchian, H. P.; Cross, J. B.; Adamo, C.; Jaramillo, J.; Gomperts, R.; Stratmann, R. E.; Yazyev, O.; Austin, A. J.; Cammi, R.; Pomelli, C.; Ochterski, J. W.; Ayala, P. Y.; Morokuma, K.; Voth, G. A.; Salvador, P.; Dannenberg, J. J.; Zakrzewski, V. G.; Dapprich, S.; Daniels, A. D.; Strain, M. C.; Farkas, O.; Malick, D. K.; Rabuck, A. D.; Raghavachari, K.; Foresman, J. B.; Ortiz, J. V.; Cui, Q.; Baboul, A. G.; Clifford, S.; Cioslowski, J.; Stefanov, B. B.; Liu, G.; Liashenko, A.; Piskorz, P.; Komaromi, I.; Martin, R. L.; Fox, D. J.; Keith, T.; Al-Laham, M. A.; Peng, C. Y.; Nanayakkara, A.; Challacombe, M.; Gill, P. M. W.; Johnson, B.; Chen, W.; Wong, M. W.; Gonzalez, C.; Pople, J. A. Gaussian 03, Revision B.04; Gaussian, Inc.: Pittsburgh, PA, 2003.

[4] Trickler, J. H.; Webb, W. W. *Opt. Lett.* **1991**, *16*, 1780-1782.

[5] Cammi, R.;Cossi, M.; Tomasi, J.; *J. Chem. Phys.* **1996**, *104*, 4611-4620.

[6] Huang, Z. L.; Lei, H.; Li, N.; Qiu, Z. R.; Wang, H. Z.; Guo, J. D.; Luo, Y.; Zhong, Z. P.; Liu, X. F.; Zhou, Z. H. *J. Mater. Chem.* **2003**, *13*, 708-711.

[7] Olsen, J.; Jorgensen, P. J. *Chem. Phys.* **1985**, *82*, 3235-3264.

[8] DALTON References in http://www.kjemi.uio.no/software/dalton/.

[9] Sun, Y. H.; Zhao, K.; Wang, C. K.; Luo, Y.; Yan, Y. X.; Tao, X. T.;Jiang, M. H. *Chem. Phys. Lett.* **2004**, *394*, 176-181.

[10] Ji, Z. Q.; Li, Y. J.; Pritchett, T. M. *et al. Chem. Eur. J.* 2011, **17**, 2479-2491

[11] Zheng, Q.; He, G. S.; Prasad, P. N.; *J. Mater. Chem.* 2005, **15**, 579-587.

[12] Li, D. M.; Zhang, Q.; Wang, P. ; Wu, J. Y.; Kan, Y. H.; Tian, Y. P.; Zhou,H. P.; Yang, J. X.; Tao, X. T.; Jiang, M. H.; *Dalton Trans*., 2011, **40**, 8170-8178.

[13] Carmichael, J.; DeGraff, W. G.; Gazdar,A. F.; Minna . J. D and Mitchell, J. B.; *Cancer Res.* **1987**, *47*, 936-942.